Designing a Planar Chiral Rhodium Indenyl Catalyst for Regio- and Enantioselective Allylic C–H Amidation

Caitlin M. B. Farr,[1,†] Amaan M. Kazerouni,[1,†] Bohyun Park,[2,3,†] Christopher D. Poff,[1,†] Joonghee Won,[2,3] Kimberly R. Sharp,[1] Mu-Hyun Baik,[3,2,*] and Simon B. Blakey[1,*]

[1]Department of Chemistry, Emory University, Atlanta, Georgia 30322, USA

[2]Department of Chemistry, Korea Advanced Institute of Science and Technology (KAIST), Daejeon 34141, Republic of Korea

[3]Center for Catalytic Hydrocarbon Functionalizations, Institute for Basic Science (IBS), Daejeon 34141, Republic of Korea

*email: sblakey@emory.edu, mbaik2805@kaist.ac.kr

Supporting Information Placeholder

ABSTRACT: Chiral variants of group IX Cp and Cp* catalysts are well established and catalyze a broad range of reactions with high levels of enantioselectivity. Enantiocontrol in these systems results from ligand design that focuses on appropriate steric blocking. Herein we report the development of a new planar chiral indenyl rhodium complex for enantioselective C–H functionalization catalysis. The ligand design is based on establishing electronic asymmetry in the catalyst, to control enantioselectivity during the reactions. The complex is easily synthesized from commercially available starting materials and is capable of catalyzing the asymmetric allylic C–H amidation of unactivated olefins, delivering a wide range of high-value enantioenriched allylic amide products in good yields with excellent regio- and enantioselectivity. Computational studies suggest that C–H cleavage is rate and enantio-determining, while reductive C–N coupling from the Rh^{V}-nitrenoid intermediate is regio-determining.

Introduction

The direct and selective functionalization of C–H bonds is a powerful and versatile transformation for organic synthesis.[1–6] Although significant advances have been made, many challenges remain unmet, particularly in the stereoselective functionalization of C(sp^3)–H bonds. Transition metal catalysis has dominated the field of asymmetric C–H functionalization driven largely by the design and development of privileged ligand classes to induce enantioselectivity.[7,8] The cyclopentadienyl (Cp) ligands are well established as one such class of privileged ligand scaffolds, as evidenced by their widespread use in transition metal catalyzed C–H functionalization.[9]

Cobalt, rhodium, and iridium cyclopentadienyl (Cp) and pentamethylcyclopentadienyl (Cp*) complexes have emerged as excellent catalysts for directed C–H functionalization, and consequently, a series of elegant chiral variants have been developed. In particular, the ligands developed by Cramer and co-workers (Figure 1A) have been used to generate a range of transition metal complexes that have exhibited exceptional capacity for enantioinduction across a broad selection of reactions.[10–13] Other notable approaches include Rovis and Ward's disclosure of an evolvable engineered streptavidin docked with biotinylated $Rh^{III}Cp^*$,[14] the amino acid derived ligands of Waldman and Antonchick,[15] and the planar chiral complex of Perekalin.[16] These seminal approaches have inspired a renewed interest in the synthesis of chiral Cp derivatives for enantioselective C–H functionalization.

Indenyl (Ind) ligands offer pronounced differences in reactivity compared to the Cp systems. Most notably, the indenyl effect,[17–19] attributed to a continuum between η^5 and η^3 binding modes of indenyl-metal complex (Figure 1B), can afford a significant acceleration in reaction rate; however, many other reactivity differences have also been observed.[20] Although the chemistry of early transition metal (Ti, Zr) indenyl complexes that exhibit planar chirality has been more thoroughly investigated, catalysis with late transition metal analogues remains largely underdeveloped. An early contribution from the Heller group describes the synthesis of a chiral pool-derived Co-complex, and its application in atroposelective heterocyclotrimerizations,[21–23] but broadly generalizable catalyst platforms are not known to date.

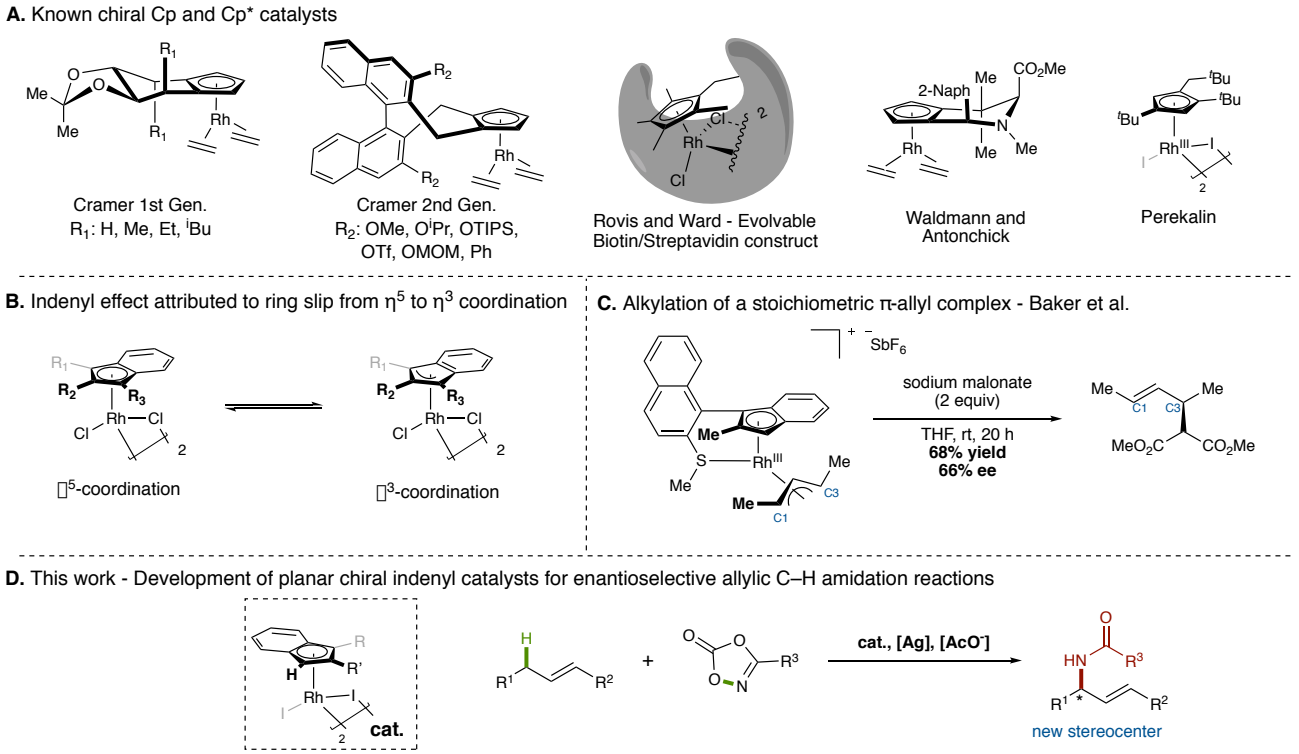

Figure 1. Enantioselective allylic C–H amidation. (A) Known chiral Cp and Cp* catalysts. (B) Ring slip of indenyl ligands from η5 to η3 binding modes. (C) Baker's alkylation of a stoichiometric π-allyl complex with sodium malonate. (D) This work – planar Rh(III)-indenyl catalysts for enantioselective allylic C–H amidation.

The frontier orbitals of the Cp and Ind ligands, depicted in Figure 2, show that the expansion of the π-orbital space from 5 to 9 MOs gives rise to two orbitals 2π and 4π in Ind that can be employed for η^5 and η^3 binding. The ring slippage of the indenyl ligand from η^5 to η^3 allows the η^3-bound carbons to exert an increased *trans*-influence, resulting in a significant electronic asymmetry.[24,25] The intrinsically asymmetric shape of the 2π MO in the 5-membered ring of the indenyl ligand plays a key role for the asymmetrization, as highlighted in red in Figure 2B. Specifically, the unsymmetrized d_{yz} orbital formed by the 2π and 4π MOs of the indenyl ligand, as marked in blue in Figure 2C, is of particular interest. We hypothesized that this electronic asymmetry could be exploited to design enantioselective catalysts. We note that electronic control has been explored in ligand design for square planar complexes using the PHOX ligands designed by Pfaltz, Helmchen, and Williams.[26–28] In the context of group IX metal complexes, Baker reported the stoichiometric reaction of a rhodium indenyl complex with sodium malonate (Figure 1C).[29] The resulting allylic substitution product was obtained in modest enantioselectivity (66% e.e.), and the sense of enantioinduction was consistent with a weakened Rh–C3 bond, arising from the aforementioned electronic asymmetry. Unfortunately, no catalysis was observed with this system, and the complexity of the ligand employed precludes systematic ligand development. Moreover, the thioether functionality presents an oxidative liability and limits its use in transformations proceeding through inner-sphere reductive C–N coupling mechanisms.

Herein, we report a class of simple modular indenyl catalysts built to leverage the electronic asymmetry in planar chiral indenyl complexes for asymmetric transformations.

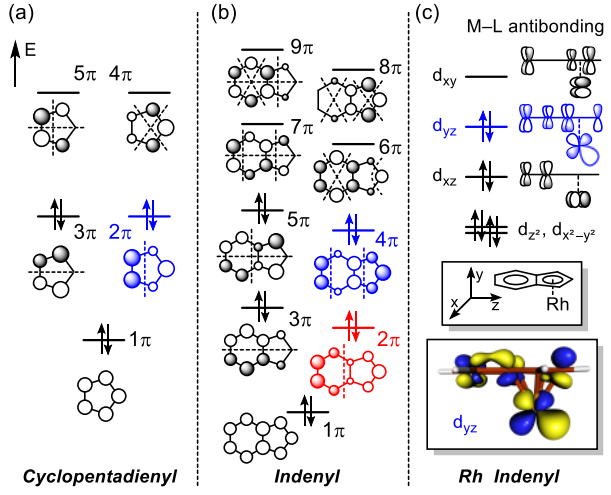

Figure 2. Qualitative molecular orbital diagram. (A) MO diagram of Cp. (B) MO diagram of Ind. (C) MO diagram of Rh-Ind made by orbital interaction between Ind and Rh.

The concept we describe herein is novel for stereoinduction and applies broadly to both inner- and outer-sphere asymmetric transformations (Figure 1D). A specific implementation is demonstrated using group IX metal-catalyzed allylic C–H functionalization via π-allyl

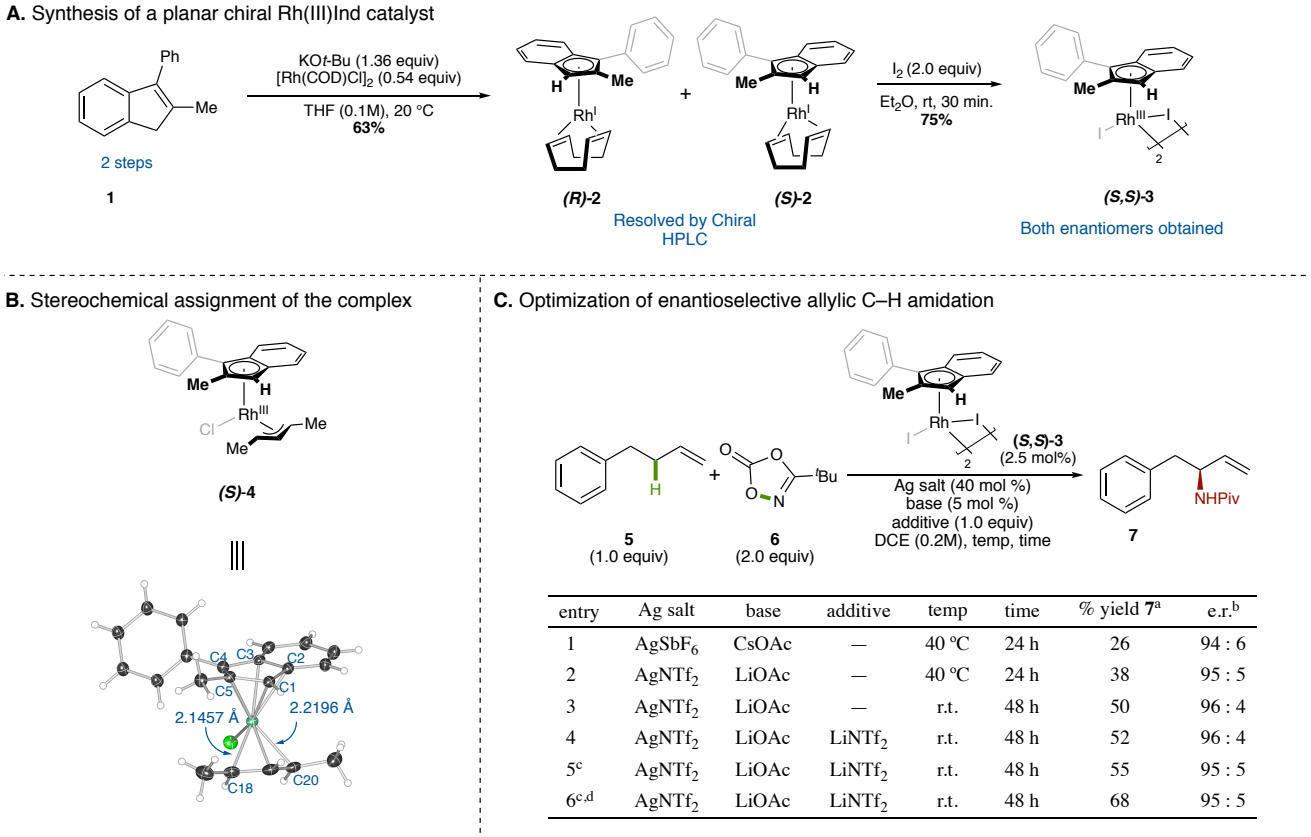

entry	Ag salt	base	additive	temp	time	% yield **7**[a]	e.r.[b]
1	$AgSbF_6$	CsOAc	—	40 °C	24 h	26	94 : 6
2	$AgNTf_2$	LiOAc	—	40 °C	24 h	38	95 : 5
3	$AgNTf_2$	LiOAc	—	r.t.	48 h	50	96 : 4
4	$AgNTf_2$	LiOAc	$LiNTf_2$	r.t.	48 h	52	96 : 4
5[c]	$AgNTf_2$	LiOAc	$LiNTf_2$	r.t.	48 h	55	95 : 5
6[c,d]	$AgNTf_2$	LiOAc	$LiNTf_2$	r.t.	48 h	68	95 : 5

Figure 3. Reaction development (A) Synthesis and chiral resolution of planar chiral Rh^{III}Ind catalyst. (B) Assignment of absolute stereochemistry of the catalyst by x-ray crystallography of its corresponding π-allyl complex of pent-2-ene. (C) Development of enantioselective allylic C–H amidation. [a]Yield determined by integration against 1,4-dinitrobenzene in crude ^{1}H NMR spectra. [b]Enantiomeric ratio was determined by chiral HPLC on OD-H column (5% isopropanol in hexanes) [c]5 mol % ***(S,S)*-3** and 10 mol % LiOAc. [d]20 mol % $AgNTf_2$.

intermediates, which is a reaction that we,[30–34] Rovis,[35–37] Glorius,[38–40] and others,[41–45] have explored previously. Due to the importance of chiral nitrogen-containing compounds,[46,47] we chose to develop and evaluate these new catalysts for the enantioselective synthesis of allylic amides[48–52] using dioxazolones as C(sp^3)–H amidating reagents,[53–56] but many other applications can be easily imagined.

Results and Discussion

Catalyst preparation and reaction optimization.

We began our exploration with a minimalistic planar chiral unit, 2-methyl-3-phenylindene **(1)**, which can be easily prepared in a modular two step synthesis from 2-methylindanone and phenyl magnesium bromide (Figure 3A).[57,58]

Complexation with [Rh(I)(COD]Cl]$_2$ provided a racemic mixture of the planar chiral COD complex **2** (63% yield), and the enantiomers were easily resolved by chiral HPLC. Each enantiomer of complex **2** was oxidized to the corresponding rhodium(III) diiodide dimer **3** (75% yield). The absolute stereochemical configuration was unambiguously assigned by x-ray crystallography of the (*S*)-π-allyl complex ***(S)*-4** (Figure 3B, see Supporting Information for details).[59] As depicted in Figure 3B, C1, C5, and C4 of the indenyl ligand in the π-allyl complex ***(S)*-4** have shorter Rh–C bonds of 2.2105 Å, 2.2225 Å, and 2.1385 Å, respectively, than C2 and C3 that display bond lengths of 2.3164 Å and 2.3106 Å, consistent with a slight slip from η^5 to η^3 binding due to the intrinsic asymmetry of the indenyl ligand. Inspection of the allyl fragment reveals a longer Rh–C20 bond (2.2196 Å) *trans* to the C1-C5-C4 moiety of the indenyl ligand compared to the Rh–C18 bond (2.1457 Å) *trans* to C2-C3. This is characteristic of the different *trans* influence exerted on two ends of the otherwise symmetrical π-allyl moiety and represents an electronic transmission of the stereochemical information from the planar chiral indenyl ligand to the allyl fragment.

With the enantioenriched rhodium indenyl complex in hand, we investigated its potential for asymmetric catalysis, probing the amidation of 4-phenylbut-1-ene **(5)** with *tert*-butyl dioxazolone (**6,** 2 equiv) using ***(S,S)*-3** as the pre-catalyst (Figure 3C). We initiated our studies using conditions identified during our discovery of the racemic allylic amidation reaction.[31] With $AgSbF_6$ (40 mol %) as the halide scavenger and CsOAc (5 mol %) as the carboxylate base, 4-phenylbut-1-ene was successfully amidated at 40 °C, providing the branched product in 26% yield and excellent enantioselectivity (94:6 e.r., entry 1, Figure 3C). The absolute stereochemical

configuration of the amidation product was established by conversion to the corresponding amino acid derivative by oxidative cleavage of the terminal olefin (see Supporting Information for details). Using $AgNTf_2$ (40 mol %) and LiOAc (5 mol %) improved the yield of **7** to 38% while maintaining the enantioselectivity (entry 2, Figure 3C). Upon lowering the reaction temperature to room temperature and extending the reaction time to 48 hours, we observed an improved yield of 50% (entry 3, Figure 3C). Based on our hypothesis that Li^+ cations might bind to the product and prevent catalyst inhibition, $LiNTf_2$ (1 equiv) was added to the reaction (entry 4, Figure 3C). Lastly, increasing the catalyst loading to 5 mol % (entry 5, Figure 3C) and decreasing the $AgNTf_2$ to 20 mol % (entry 6, Figure 3C) further improved the reaction, providing the pivalamide product **7** in 68% yield and 95:5 e.r.

Scope and limitations.

Under optimized conditions, the simple feedstock olefin 4-methylpent-1-ene was effectively amidated with a wide range of dioxazolone substrates. Methyl, *tert*-butyl, cyclohexyl and benzyl dioxazolone all provided the corresponding amide products (**9-12**, respectively) in moderate to good yields (55-77%) and excellent enantioselectivity (95:5 - >99:1, Figure 4).

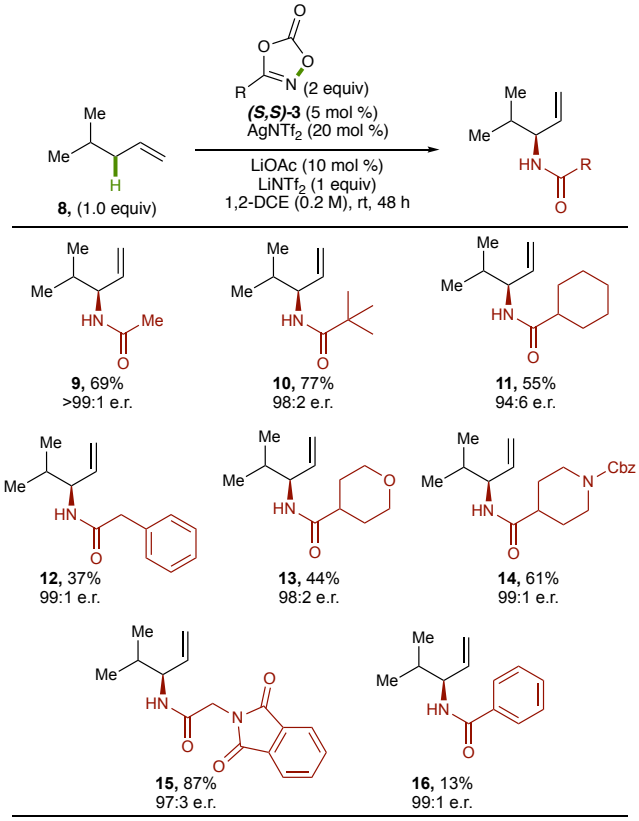

Figure 4. Scope of dioxazolone substrates for enantioselective allylic C–H amidation. Reactions were run on 0.10 mmol scale. Isolated yields are reported, and enantiomeric ratios were determined by chiral HPLC (see Supporting Information for details).

The reaction was tolerant of ether and carbamate functionality on the dioxazolone substrate, providing amides **13** and **14** in 44% and 61% yield and 98:2 and 99:1 e.r. respectively. Phthaloyl-glycine-derived dioxazolone provided the amide product **15** in 87% yield and 97:3 e.r., highlighting the applicability of amino acid derived dioxazolones in this methodology. Phenyl dioxazolone, however, only provided the amide product **16** in 13% yield, albeit with high enantioselectivity (99:1 e.r.). The observation that aryl dioxazolones provide lower yields in these reactions is consistent with the data from previous racemic reactions with $RhCp^*$ and $IrCp^*$ catalysts.[31,35,39]

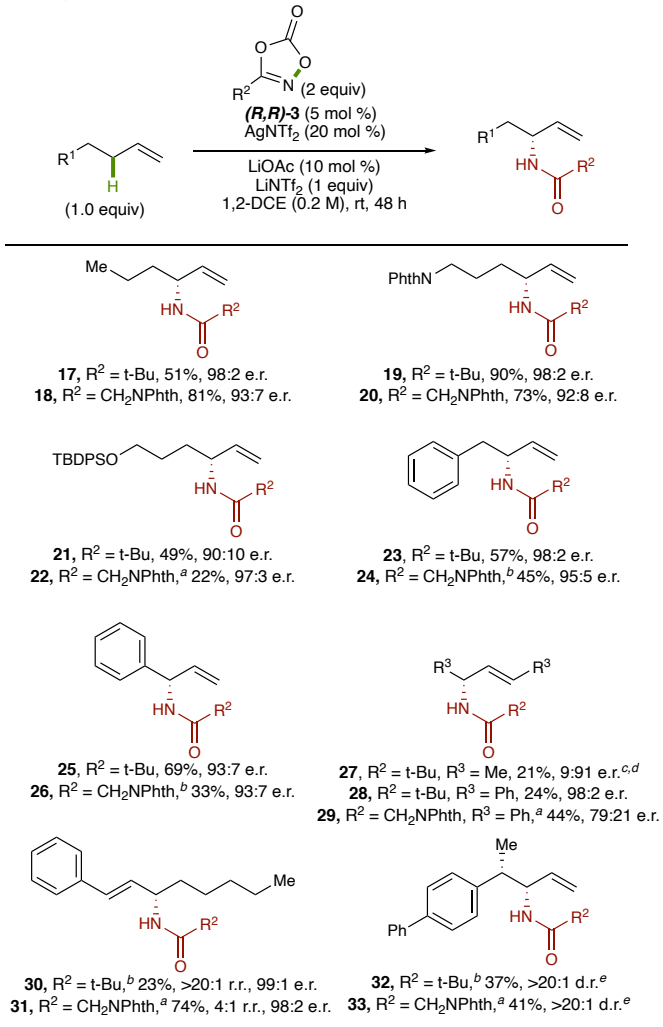

Figure 5. Scope of olefin substrates for enantioselective allylic C–H amidation. Isolated yields are reported and enantiomeric ratios were determined by chiral HPLC (see Supporting Information for details). [a]Reaction run at 60 °C. [b]Reaction run at 40 °C. [c]***(S,S)*-3** used as the precatalyst. [d]Major enantiomer has *(S)*-stereochemistry. [e]Diastereomeric ratio determined by integration of ^1H NMR spectra.

To establish the compatibility of this reaction with an array of olefins, we chose *tert*-butyl dioxazolone and *N*-Phth-glycine dioxazolone, as representatives of electron-rich and electron-poor substrates, respectively (Figure 5). When the reaction was performed on the simple straight chain olefin hex-1-ene, the branched amide product **17**

was isolated in 51% yield and 98:2 e.r. with *tert*-butyl dioxazolone, while amide **18** was isolated in 81% yield and 93:7 e.r. with phthaloyl-glycine dioxazolone. The reaction performed well on *N*-phthalimide hex-1-ene, providing the amide products with both *tert*-butyl and phthaloyl-glycine dioxazolone in good yield and enantioselectivity (**19,** 90% yield, 98:2 e.r. and **20,** 73% yield, 92:8 e.r., respectively). Amide **21**, bearing a silyloxy substituent, was isolated in 49% yield and 90:10 e.r. when the reaction was conducted with *tert*-butyl dioxazolone. However, elevated temperatures were required to provide amide product **22** (22% yield, 97:3 e.r.) with phthaloyl-glycine dioxazolone. The allylic amidation was also successful on 4-phenylbut-1-ene, providing amides **23** and **24** in 57% yield, 98:2 e.r. and 45% yield, 95:5 e.r., respectively. No olefin isomerization was observed. Amidations of allylbenzenes were successful, providing amides **25** (69% yield, 93:7 e.r.) and **26** (33% yield, 93:7 e.r.). Importantly, good enantioselectivity was observed when the reaction was performed on 2-pentene and 1,3-diphenylpropene, both of which proceed through ostensibly symmetrical π-allyl intermediates (**27**, 21% yield, 91:9 e.r., **28**, 24% yield, 98:2 e.r. and **29**, 44% yield, 79:21 e.r.). These results support our hypothesis that enantioinduction in this reaction may result from electronic asymmetry transmitted from the indenyl ligand to the allyl fragment rather than purely a steric phenomenon. We note that an unsymmetrical internal styrenyl olefin is also tolerated, and amides were obtained both regio- and stereoselectively. The reaction is regioselective for the conjugated amide products, delivering pivalamide **30** in 23% yield (>20:1 r.r., 99:1 e.r.) and amide **31** in 74% yield (4:1 r.r., 98:2 e.r.). For both disubstituted olefins, the more sterically demanding *tert*-butyl dioxazolone resulted in lower yields than the *N*-Phth-glycine dioxazolone, suggesting that steric crowding may begin to become limiting in these scenarios. The reaction also displays excellent diastereoselectivity when performed on a matched enantioenriched homoallylic stereogenic substrate.[60] With the (*R,R)* pre-catalyst and the *(R)*-substrate, we isolated the expected amide products **32** and **33** in 37% and 41% yields, respectively, with >20:1 d.r. as determined by ^{1}H NMR. However, when these reactions were performed under the same conditions but with the *(S,S)* pre-catalyst (mismatched), no reaction occurred and the starting dioxazolones and olefins were recovered in high yield. We anticipate that a broader family of planar chiral indenyl catalysts will be essential to address cases of matched *vs* mismatched allylic C–H amidation.

While studying the scope of this reaction, we observed that more Lewis basic dioxazolones (i.e. dioxazolones with more electron donating R groups) performed generally better at lower temperatures. Consistent with this observation, *tert*-butyl dioxazolone generally delivered the corresponding amide products in higher yields when the reactions were performed at room temperature. In contrast, *N*-Phth-glycine dioxazolone, (with an inductively electron withdrawing R group) was able to tolerate, and in some cases, required elevated temperatures to deliver the amide product. We speculate that more Lewis basic dioxazolones can coordinate to the rhodium complex competitively with π-allyl formation, leading to deleterious side reactions and catalyst arrest. In these cases, lower reaction temperatures are required to exacerbate selectivity for the productive pathway.

Reaction mechanism.

Having established the broad applicability of this reaction, we turned our attention to its mechanism. Stoichiometric and kinetic investigations of $Ir^{III}Cp^*$- and $Rh^{III}Cp^*$-catalyzed allylic C–H amidation have been previously reported by us and Rovis.[31,35] The isolation and characterization of $Rh^{III}Cp^*$- and $Ir^{III}Cp^*$-π-allyl complexes suggest the presence of these intermediates in the operative catalytic cycle, as opposed to direct insertion of a metallonitrene species into the allylic C–H bond. This is further supported by regioconvergent allylic amidation of isomeric olefin substrates as demonstrated by Glorius and coworkers,[39] as well the regioisomeric product mixtures observed when this reaction occurs on 1,2-disubstituted olefins.[31,39] Additionally, intra- and intermolecular isotopic competition experiments reported by the Rovis group[35] indicate that C–H activation is irreversible and C–H cleavage may be involved in the rate-determining step of this reaction.

Density functional theory calculations were carried out to establish a plausible mechanism and elucidate the origin of the regio- and enantioselectivity.[61] Figure 6 shows a complete energy profile for the *(R,R)*-[Rh(2-Me-3-Ph-Ind)I_2]$_2$-catalyzed allylic C–H amidation of allylbenzene with *tert*-butyl dioxazolone. While olefin coordination to the cationic rhodium complex **A** is reversible, allowing it to bind the catalyst on both faces (**B** and **B'**), the subsequent allylic C–H activation step that proceeds via a concerted-metalation-deprotonation (CMD) mechanism is likely rate-limiting with the barriers being 18.8 and 19.9 kcal/mol, respectively. The asymmetric indenyl ligand favors **B-TS**, where two phenyl moieties of the ligand and the olefin substrate point away from each other, as illustrated in Figure 6. The alternative transition state **B'-TS** is 1.1 kcal/mol higher energy. These two transition states lead to the π-allyl complexes **C** and **C'**, where the enantioselectivity of the reaction has been initially determined, as the subsequent steps preserve the stereochemical information set at this stage. After dissociative loss of acetic acid, one equiv. of the *tert*-butyl dioxazolone binds to the metal center, where two different conformations are possible.

In the isomer **E** the *tert*-butyl group is oriented *syn* to the π-allyl functionality, whereas in **E"** the *tert*-butyl group is aligned *syn* to the phenyl group of the π-allyl. Both isomers could potentially proceed to release CO_2

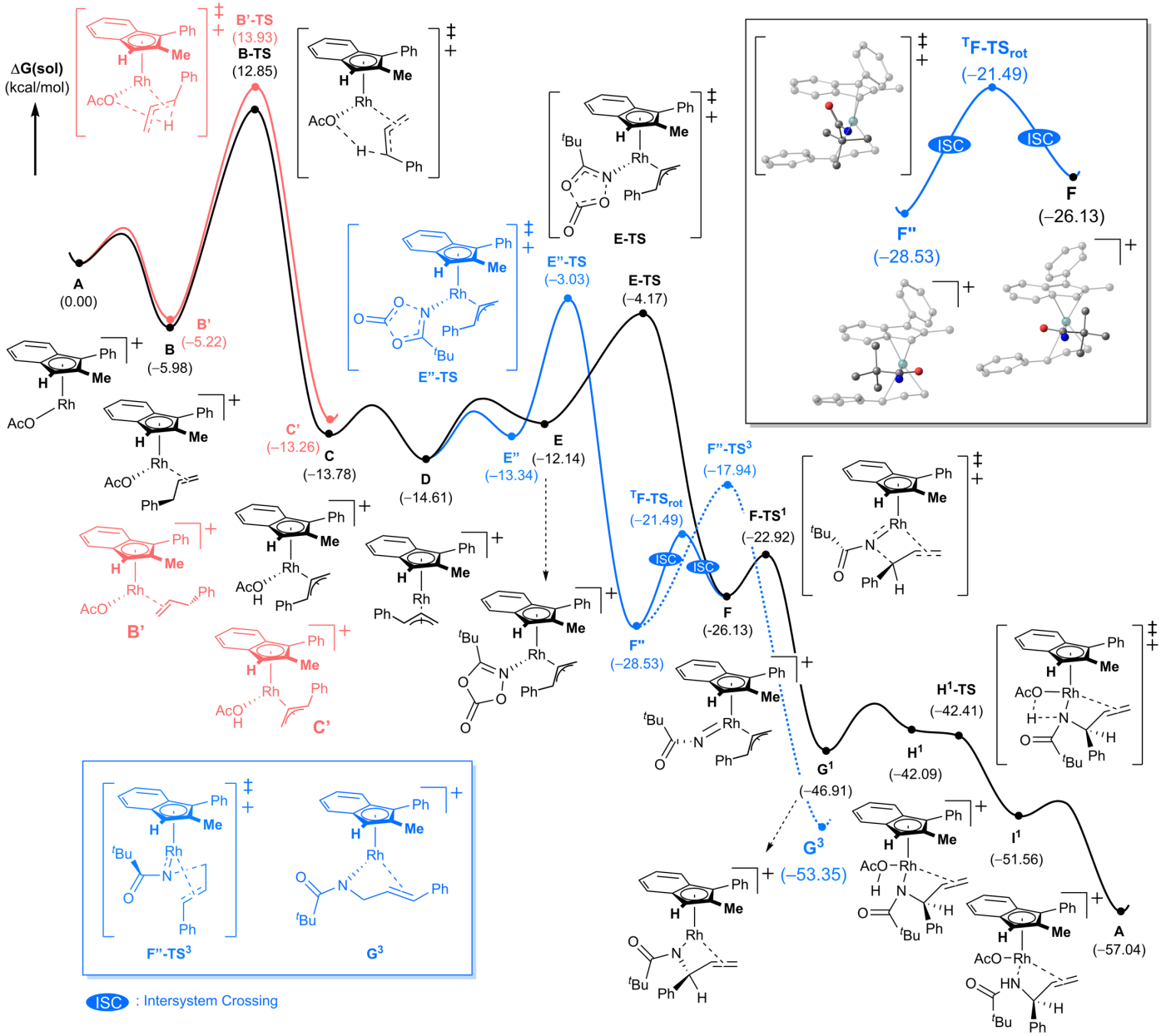

Figure 6. Complete energy profile diagram for the enantioselective amidation of allylbenzene with *tert*-butyl dioxazolone.

and irreversibly form the imido complexes **F** and **F"**, traversing the transition states **E-TS** and **E"-TS**, respectively. As the metal-imido complex is known to readily access the triplet state,[62] the interconversion between **F** and **F"** *via* a triplet transition state, **^{T}F-TS$_{rot}$** should be possible. Thus, the regioselectivity is determined at the reductive C–N coupling step.

Curiously, the energy difference between the two transition states **F-TS^{1}** and **F"-TS^{3}** is remarkably large at 5.0 kcal/mol and is responsible for the kinetic preference of the regioisomer **G^{1}** over the thermodynamically preferred alternative **G^{3}**.

This difference originates from the asymmetric character of the indenyl ligand. Because of the different *trans*-influence of the ligand as mentioned above and highlighted in Figures 2C and 3B, the allylic C1-carbon

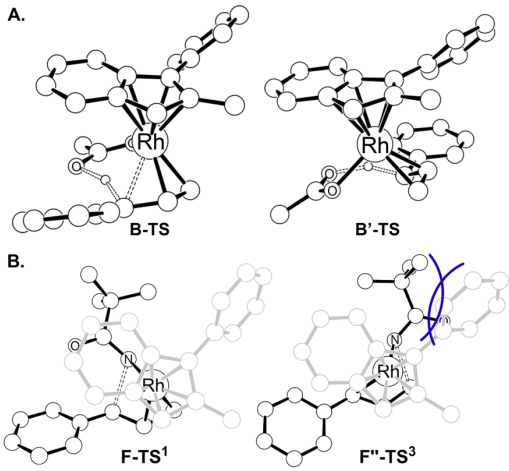

Figure 7. Optimized structures of (A) **B-TS** and **B'-TS**, and (B) **F-TS^{1}** and **F"-TS^{3}**. Non-essential atoms have been omitted for clarity

forms a weaker Rh–C bond, and is more easily attacked by the imido-nitrogen than the C3-carbon. Moreover, the phenyl substituent on the indenyl ligand further increases the enantioselectivity. As shown in Figure 7, the imide intermediate **F** can access to the benzylic carbon with almost no steric hindrance through the transition state **F-TS[1]**, while much higher steric demand between bulky *tert*-butyl group and phenyl moiety blocks imide from approaching the terminal carbon in **F''-TS[3]**. Therefore, the imide preferably attacks the branched allylic carbon on the opposite side from the indenyl phenyl, which has a bigger substituent than the other carbon. An energy decomposition analysis of the two transition states in support of this interpretation is given in the supporting information.

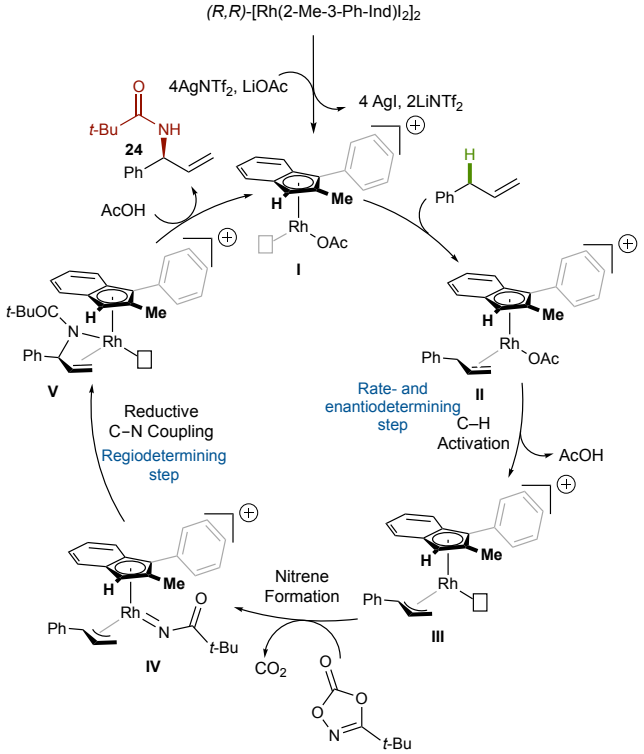

Figure 8. Proposed catalytic cycle based on computational and experimental analyses.

Based on our computational studies and experimental observations, along with previously reported stoichiometric investigations,[31,36] we propose the catalytic cycle shown in Figure 8. The dimeric precatalyst ***(R,R)*-3** is activated by $AgNTf_2$ and LiOAc to form the coordinatively unsaturated cationic indenyl complex **I**. Following coordination of the olefin, complex **II** can undergo rate- and enantiodetermining C–H cleavage to form π-allyl complex **III**. The dioxazolone can then coordinate the complex at the vacant coordination site, followed by CO_2 expulsion to produce the imido complex **IV**, which quickly undergoes regio-determining reductive coupling to form the allylic C–N bond at the branched position of the π-allyl. Protodemetalation of complex **V** and coordination of acetate produces the desired product while regenerating the active catalyst **I**.

In this mechanism, the dioxazolone substrate adds to the Rh-center after the completion of the enantioselective C–H activation step. Because the experimental work showed measurable differences in the degree of enantioselectivity as different dioxazolones are employed, one may consider a more prominent role of the dioxazolone in determining the stereochemical outcome. However, the differences enumerated in Figure 5, such as an e.r. of 90:10 vs. 97:3 when dioxazolones with R^2 = t-Bu and R^2 = CH_2NPhth are used, respectively, are much too small to be captured as meaningful barrier differences in our calculations. The proposed role of the dioxazolone for the enantioselectivity is that it arrests both enantiomers that are formed by the C–H activation step and carries them through the nitrene formation and C–N coupling steps. Our calculations indicate that the formation of the experimentally observed enantiomer **C** is kinetically preferred by ~1 kcal/mol over **C'**, which translates to a preference of ~10:1. It is easy to envision that the engagement and the efficiency of these steps vary with the exact nature of the dioxazolone substrate, leading to a detectable difference in the e.r. of the final product. These minute differences in the mechanism cannot be properly reproduced with currently available molecular modelling techniques.

Conclusion

We have described the development of a novel planar chiral rhodium indenyl complex for regio- and enantioselective amidation of allylic C–H bonds. The rhodium pre-catalyst can be quickly synthesized from readily available starting materials. The reaction exhibits wide functional group compatibility, providing an array of enantioenriched allylic amide products from readily available alkene starting materials, including feedstock olefins like hex-1-ene and 4-methylpent-1-ene. Crystallographic evidence supports the electronic transmission of asymmetry from the planar chiral indenyl ligand to the π-allyl ligand in a key intermediate in the catalytic cycle. Computational studies indicate that C–H cleavage to form the π-allyl complex is turnover limiting and enantio-determining. The reductive elimination from the key Rh^V-nitrenoid complex is regio-determining and occurs at the weaker Rh–C bond, with the differing Rh–C bond strengths resulting from the electronic asymmetry established by the indenyl ligand. The computational studies also demonstrate that steric interactions contribute to both these steps. Current work is directed towards synthesizing a library of planar chiral group IX complexes which we anticipate will have broad applicability in mechanistically distinct asymmetric transformations.

ASSOCIATED CONTENT

The Supporting Information is available free of charge on the ACS Publications website.

Methods and Materials, characterization data (PDF, CIF)

AUTHOR INFORMATION

Corresponding Authors

Simon B. Blakey - Department of Chemistry, Emory University, Atlanta, Georgia 30322, USA; 0000-0002-4100-8610

Mu-Hyun Baik - Center for Catalytic Hydrocarbon Functionalizations, Institute for Basic Science (IBS), Daejeon 34141, Republic of Korea; Department of Chemistry, Korea Advanced Institute of Science and Technology (KAIST), Daejeon 34141, Republic of Korea; 0000-0002-8832-8187

Authors

Caitlin M. B. Farr - Department of Chemistry, Emory University, Atlanta, Georgia 30322, USA; 0000-0002-3289-1528

Amaan M. Kazerouni - Department of Chemistry, Emory University, Atlanta, Georgia 30322, USA; 0000-0002-4121-2603

Bohyun Park - Department of Chemistry, Korea Advanced Institute of Science and Technology (KAIST), Daejeon 34141, Republic of Korea; Center for Catalytic Hydrocarbon Functionalizations, Institute for Basic Science (IBS), Daejeon 34141, Republic of Korea; 0000-0003-0552-8763

Christopher D. Poff - Department of Chemistry, Emory University, Atlanta, Georgia 30322, USA; 0000-0001-8000-7525

Joonghee Won - Department of Chemistry, Korea Advanced Institute of Science and Technology (KAIST), Daejeon 34141, Republic of Korea; Center for Catalytic Hydrocarbon Functionalizations, Institute for Basic Science (IBS), Daejeon 34141, Republic of Korea; 0000-0002-2487-8788

Kimberly R. Sharp - Department of Chemistry, Emory University, Atlanta, Georgia 30322, USA; 0000-0002-5718-3552

Author Contributions

†C. M. B. F., A. M. K., B. P., and C. D. P. contributed equally and are listed alphabetically by surname.

Notes

The authors declare no competing interests.

ACKNOWLEDGMENT

The research was supported in part by the Institute for Basic Science (IBS-R10-A1) in South Korea, the National Science Foundation (NSF) under the CCI Center for Selective C−H Functionalization (CHE-1700982), and the American Chemical Society Petroleum Research Fund (ACS-PRF-59563-ND1). NMR studies for this research were performed on instrumentation funded by the NSF (CHE-1531620). The X-ray analysis was done by the Emory X-ray Crystallography Facility using the Rigaku Synergy-S diffractometer, supported by the NSF (CHE-1626172). We gratefully acknowledge Dr. John Bacsa for x-ray crystallographic analysis of compound **4** and the Liotta group for use of their chiral semi-prep HPLC.

REFERENCES

(1) Gutekunst, W. R.; Baran, P. S. C-H Functionalization Logic in Total Synthesis. *Chem. Soc. Rev*. **2011**, *40*, 1976–1991.

(2) Godula, K.; Sames, D. C-H Bond Functionalization in Complex Organic Synthesis. *Science*. **2006**, *312*, 67–72.

(3) Noisier, A. F. M.; Brimble, M. A. C-H Functionalization in the Synthesis of Amino Acids and Peptides. *Chem. Rev.* **2014**, *114*, 8775–8806.

(4) Yamaguchi, J.; Yamaguchi, A. D.; Itami, K. C-H Bond Functionalization: Emerging Synthetic Tools for Natural Products and Pharmaceuticals. *Angew. Chem. Int. Ed*. **2012**, *51*, 8960–9009.

(5) Davies, H. M. L.; Du Bois, J.; Yu, J. Q. C-H Functionalization in Organic Synthesis. *Chem. Soc. Rev*. **2011**, *40*, 1855–1856.

(6) Ye, J.; Lautens, M. Palladium-Catalysed Norbornene-Mediated C–H Functionalization of Arenes. *Nat. Chem.* **2015,** *7,* 863–870.

(7) Newton, C. G.; Wang, S.-G.; Oliveira, C. C.; Cramer, N. Catalytic Enantioselective Transformations Involving C–H Bond Cleavage by Transition-Metal Complexes. *Chem. Rev.* **2017**, *117*, 8908–8976.

(8) Loup, J.; Dhawa, U.; Pesciaioli, F.; Wencel-Delord, J.; Ackermann, L. Enantioselective C−H Activation with Earth-Abundant 3d Transition Metals. *Angew. Chem. Int. Ed.* **2019**, *58*, 12803–12818.

(9) Zhu, R. Y.; Farmer, M. E.; Chen, Y. Q.; Yu, J. Q. A Simple and Versatile Amide Directing Group for C−H Functionalizations. *Angew. Chem. Int. Ed*. **2016**, *55*, 10578–10599.

(10) Ye, B.; Cramer, N. A Tunable Class of Chiral Cp Ligands for Enantioselective Rhodium(III)-Catalyzed C–H Allylations of Benzamides. *J. Am. Chem. Soc.* **2013**, *135* , 636–639.

(11) Ye, B.; Cramer, N. Chiral Cyclopentadienyl Ligands as Stereocontrolling Element in Asymmetric C-H

Functionalization. *Science* **2012**, *338*, 504–506.

(12) Ye, B.; Cramer, N. Chiral Cyclopentadienyls: Enabling Ligands for Asymmetric Rh(III)-Catalyzed C-H Functionalizations. *Acc. Chem. Res.* **2015**, *48*, 1308–1318.

(13) Newton, C. G.; Kossler, D.; Cramer, N. Asymmetric Catalysis Powered by Chiral Cyclopentadienyl Ligands. *J. Am. Chem. Soc.* **2016**, *128*, 3935–3941.

(14) Hyster, T. K.; Knörr, L.; Ward, T. R.; Rovis, T. Biotinylated Rh(III) Complexes in Engineered Streptavidin for Accelerated Asymmetric C-H Activation. *Science* **2012**, *338*, 500–503.

(15) Jia, Z.-J. J.; Merten, C.; Gontla, R.; Daniliuc, C. G.; Antonchick, A. P.; Waldmann, H. General Enantioselective C−H Activation with Efficiently Tunable Cyclopentadienyl Ligands. *Angew. Chem. Int. Ed.* **2017**, *56*, 2429–2434.

(16) Trifonova, E. A.; Ankudinov, N. M.; Mikhaylov, A. A.; Chusov, D. A.; Nelyubina, Y. V.; Perekalin, D. S. A Planar-Chiral Rhodium(III) Catalyst with a Sterically Demanding Cyclopentadienyl Ligand and Its Application in the Enantioselective Synthesis of Dihydroisoquinolones. *Angew. Chem. Int. Ed.* **2018**, *57*, 7714–7718.

(17) Marder, T. B.; Calabrese, J. C.; Roe, D. C.; Tulip, T. H. The Slip-Fold Distortion of .Pi.-Bound Indenyl Ligands. Dynamic NMR and x-Ray Crystallographic Studies of (.Eta.-Indenyl)RhL2 Complexes. *Organometallics* **1987**, *6*, 2012–2014.

(18) Hart-Davis, A. J.; Mawby, R. J. Reactions of π-Indenyl Complexes of Transition Metals. Part I. Kinetics and Mechanisms of Reactions of Tricarbonyl-π-Indenylmethylmolybdenum with Phosphorus(III) Ligands. *J. Chem. Soc. A* **1969**, 2403–2407.

(19) Westcott, S. A.; Kakkar, A. K.; Stringer, G.; Taylor, N. J.; Marder, T. B. Flexible Coordination of Indenyl Ligands in Sandwich Complexes of Transition Metals. Molecular Structures of [(η-C9R7)2M] (M = Fe, R = H, Me; M = Co, Ni, R = H): Direct Measurement of the Degree of Slip-Fold Distortion as a Function of d-Electron Count. *J. Organomet. Chem.* **1990**, *394*, 777–794.

(20) Trost, B. M.; Ryan, M. C. Indenylmetal Catalysis in Organic Synthesis. *Angew. Chem. Int. Ed*. **2017**, *56*, 2862–2879.

(21) Hapke, M.; Kral, K.; Fischer, C.; Spannenberg, A.; Gutnov, A.; Redkin, D.; Heller, B. Asymmetric Synthesis of Axially Chiral 1-Aryl-5,6,7,8-Tetrahydroquinolines by Cobalt-Catalyzed [2 + 2 + 2] Cycloaddition Reaction of 1-Aryl-1,7-Octadiynes and Nitriles. *J. Org. Chem.* **2010**, *75*, 3993–4003.

(22) Heller, B.; Gutnov, A.; Fischer, C.; Drexler, H. J.; Spannenberg, A.; Redkin, D.; Sundermann, C.; Sundermann, B. Phosphorus-Bearing Axially Chiral Biaryls by Catalytic Asymmetric Cross-Cyclotrimerization and a First Application in Asymmetric Hydrosilylation. *Chem. Eur. J.* **2007**, *13* , 1117–1128.

(23) Gutnov, A.; Heller, B.; Fischer, C.; Drexler, H. J.; Spannenberg, A.; Sundermann, B.; Sundermann, C. Cobalt(I)-Catalyzed Asymmetric [2+2+2] Cycloaddition of Alkynes and Nitriles: Synthesis of Enantiomerically Enriched Atropoisomers of 2-Arylpyridines. *Angew. Chem. Int. Ed.* **2004**, *43*, 3795–3797.

(24) Rerek, M. E.; Ji, L. N.; Basolo, F. The Indenyl Ligand Effect on the Rate of Substitution Reactions of $Rh(\eta\text{-}C_9H_7)(CO)_2$ and $Mn(\eta\text{-}C_9H_7)(CO)_3$. *J. Chem. Soc. Chem. Commun.* **1983**, 1208–1209.

(25) Rerek, M. E.; Basolo, F. Kinetics and Mechanism of the Substitution Reactions of (H5-Pentamethylcyclopentadienyl)Dicarbonylrhodium(I) and (H5-Pentamethylcyclopentadienyl)Dicarbonylcoball(I). *Organometallics* **1983**, *2*, 372–376.

(26) Dawson, G. J.; Frost, C. G.; Williams, J. M. J.; Coote, S. J. Asymmetric Palladium Catalysed Allylic Substitution Using Phosphorus Containing Oxazoline Ligands. *Tetrahedron Lett.* **1993**, *34*, 3149–3150.

(27) Sprinz, J.; Helmchen, G. Phosphinoaryl- and Phosphinoalkyloxazolines as New Chiral Ligands for Enantioselective Catalysis: Very High Enantioselectivity in Palladium Catalyzed Allylic Substitutions. *Tetrahedron Lett.* **1993**, *34*, 1769–1772.

(28) von Matt, P.; Pfaltz, A. Chiral Phosphinoaryldihydrooxazoles as Ligands in Asymmetric Catalysis: Pd-Catalyzed Allylic Substitution. *Angew. Chem. Int. Ed. Engl.* **1993**, *32*, 566–568.

(29) Baker, R. W. Asymmetric Induction via the Structural Indenyl Effect. *Organometallics* **2018**, *37*, 433–440.

(30) Harris, R. J.; Park, J.; Nelson, T. A. F.; Iqbal, N.; Salgueiro, D. C.; Bacsa, J.; MacBeth, C. E.; Baik, M. H.; Blakey, S. B. The Mechanism of Rhodium-Catalyzed Allylic C-H Amination. *J. Am. Chem. Soc.* **2020**, *142*, 5842–5851.

(31) Burman, J. S.; Harris, R. J.; B. Farr, C. M.; Bacsa, J.; Blakey, S. B. Rh(III) and Ir(III)Cp* Complexes Provide Complementary Regioselectivity Profiles in Intermolecular Allylic C–H Amidation Reactions. *ACS Catal.* **2019**, *9*, 5474–5479.

(32) Kazerouni, A. M.; Nelson, T. A. F.; Chen, S. W.; Sharp, K. R.; Blakey, S. B. Regioselective Cp*Ir(III)-Catalyzed Allylic C–H Sulfamidation of Allylbenzene Derivatives. *J. Org. Chem.* **2019**, *84*, 13179–13185.

(33) Nelson, T. A. F.; Blakey, S. B. Intermolecular Allylic C−H Etherification of Internal Olefins. *Angew. Chem. Int. Ed.* **2018**, *57*, 14911–14915.

(34) Burman, J. S.; Blakey, S. B. Regioselective Intermolecular Allylic C−H Amination of Disubstituted Olefins via Rhodium/π-Allyl Intermediates. *Angew. Chem. Int. Ed.* **2017**, *56*, 13666–13669.

(35) Lei, H.; Rovis, T. Ir-Catalyzed Intermolecular Branch-Selective Allylic C-H Amidation of Unactivated Terminal Olefins. *J. Am. Chem. Soc.* **2019**, *141*, 2268–2273.

(36) Lei, H.; Rovis, T. A Site-Selective Amination Catalyst Discriminates between Nearly Identical C–H Bonds of Unsymmetrical Disubstituted Alkenes. *Nat. Chem.* **2020**, 1–7. https://doi.org/10.1038/s41557-020-0470-z.

(37) Archambeau, A.; Rovis, T. Rhodium(III)-Catalyzed Allylic C(sp^3)–H Activation of Alkenyl Sulfonamides: Unexpected Formation of Azabicycles. *Angew. Chem. Int. Ed.* **2015**, *54*, 13337–13340.

(38) Knecht, T.; Pinkert, T.; Dalton, T.; Lerchen, A.; Glorius, F. Cp*Rh^{III}-Catalyzed Allyl–Aryl Coupling of Olefins and Arylboron Reagents Enabled by C(sp^3)–H Activation. *ACS Catal.* **2019**, *9*, 1253–1257.

(39) Knecht, T.; Mondal, S.; Ye, J.-H.; Das, M.; Glorius, F. Intermolecular, Branch-Selective, and Redox-Neutral Cp*Ir^{III} -Catalyzed Allylic C−H Amidation. *Angew. Chem. Int. Ed.* **2019**, *58*, 7117–7121.

(40) Lerchen, A.; Knecht, T.; Koy, M.; Ernst, J. B.; Bergander, K.; Daniliuc, C. G.; Glorius, F. Non-Directed Cross-Dehydrogenative (Hetero)Arylation of Allylic C(sp^3)−H Bonds Enabled by C−H Activation. *Angew. Chem. Int. Ed.* **2018**, *57*, 15248–15252.

(41) Sihag, P.; Jeganmohan, M. Iridium(III)-Catalyzed Intermolecular Allylic C-H Amidation of Internal Alkenes with Sulfonamides. *J. Org. Chem.* **2019**, *84*, 13053–13064.

(42) Liu, Y.; Yang, Y.; Wang, C.; Wang, Z.; You, J. Rhodium(III)-Catalyzed Regioselective Oxidative Annulation of Anilines and Allylbenzenes: Via C(sp^3)-H/C(sp^2)-H Bond Cleavage. *Chem. Commun.* **2019**, *55*, 1068–1071.

(43) Sun, J.; Wang, K.; Wang, P.; Zheng, G.; Li, X. Rhodium(III)-Catalyzed Oxidative Allylic C-H Indolylation via Nucleophilic Cyclization. *Org. Lett.* **2019**, *21*, 4662–4666.

(44) Shibata, Y.; Kudo, E.; Sugiyama, H.; Uekusa, H.; Tanaka, K. Facile Generation and Isolation of φ-Allyl Complexes from Aliphatic Alkenes and an Electron-Deficient Rh(III) Complex: Key Intermediates of Allylic C–H Functionalization. *Organometallics* **2016**, *35* (10), 1547–1552.

(45) Cochet, T.; Bellosta, V.; Roche, D.; Ortholand, J. Y.; Greiner, A.; Cossy, J. Rhodium(Iii)-Catalyzed Allylic C-H Bond Amination. Synthesis of Cyclic Amines from ω-Unsaturated N-Sulfonylamines. *Chem. Commun.* **2012**, *48*, 10745–10747.

(46) *Stereoselective Formation of Amines*; Li, W., Zhang, X., Eds.; Topics in Current Chemistry; Springer Berlin Heidelberg: Berlin, Heidelberg, 2014; Vol. 343.

(47) Nugent, T. C.; El-Shazly, M. Chiral Amine Synthesis - Recent Developments and Trends for Enamide Reduction, Reductive Amination, and Imine Reduction. *Adv. Synth. Catal*. **2010**, 753–819.

(48) Liang, C.; Collet, F.; Robert-Peillard, F.; Müller, P.; Dodd, R. H.; Dauban, P. Toward a Synthetically Useful Stereoselective C-H Amination of Hydrocarbons. *J. Am. Chem. Soc.* **2008**, *130*, 343–350.

(49) Bao, H.; Tambar, U. K. Catalytic Enantioselective Allylic Amination of Unactivated Terminal Olefins via an Ene Reaction/[2,3]-Rearrangement. *J. Am. Chem. Soc.* **2012**, *134*, 18495–18498.

(50) Bayeh, L.; Le, P. Q.; Tambar, U. K. Catalytic Allylic Oxidation of Internal Alkenes to a Multifunctional Chiral Building Block. *Nature* **2017**, *547*, 196–200.

(51) Robak, M. T.; Herbage, M. A.; Ellman, J. A. Synthesis and Applications of Tert - Butanesulfinamide. *Chem. Rev.* **2010**, *110*, 3600–3740.

(52) Jiang, G.; Halder, R.; Fang, Y.; List, B. A Highly Enantioselective Overman Rearrangement through Asymmetric Counteranion-Directed Palladium Catalysis. *Angew. Chem. Int. Ed.* **2011**, *50*, 9752–9755.

(53) Tan, P. W.; Mak, A. M.; Sullivan, M. B.; Dixon, D. J.; Seayad, J. Thioamide-Directed Cobalt(III)-Catalyzed Selective Amidation of C(sp^3)−H Bonds. *Angew. Chem. Int. Ed.* **2017**, *56*, 16550–16554.

(54) Shi, H.; Dixon, D. J. Dithiane-Directed Rh(III)-Catalyzed Amidation of Unactivated C(sp^3)-H Bonds. *Chem. Sci.* **2019**, *10*, 3733–3737.

(55) Wang, H.; Park, Y.; Bai, Z.; Chang, S.; He, G.; Chen, G. Iridium-Catalyzed Enantioselective C(sp^3)−H Amidation Controlled by Attractive Noncovalent Interactions. *J. Am. Chem. Soc.* **2019**, *141*, 7194–7201.

(56) Hong, S. Y.; Park, Y.; Hwang, Y.; Kim, Y. B.; Baik, M.-H.; Chang, S. Selective Formation of γ-Lactams via C–H Amidation Enabled by Tailored Iridium Catalysts. *Science* **2018**, *359*, 1016–1021.

(57) Biosca, M.; Salomó, E.; de la Cruz-Sánchez, P.; Riera, A.; Verdaguer, X.; Pàmies, O.; Diéguez, M. Extending the Substrate Scope in the Hydrogenation of Unfunctionalized Tetrasubstituted Olefins with Ir-P Stereogenic Aminophosphine–Oxazoline Catalysts. *Org. Lett.* **2019**, *21*, 807–811.

(58) Nalesnik, T. E.; Freudenberger, J. H.; Orchin, M. Hydrogenation Reactions with Hydridocobalt Tetracarbonyl. *J. Organomet. Chem.* **1981**, *221*, 193–197.

(59) Schlögl, K. Stereochemistry of Metallocenes. 20 Years of Progress and Recent Advances. *J. Organomet. Chem.* **1986**, *300*, 219–248.

(60) Wang, Y. M.; Buchwald, S. L. Enantioselective CuH-Catalyzed Hydroallylation of Vinylarenes. *J. Am. Chem. Soc.* **2016**, *138*, 5024–5027.

(61) Geometry optimization, vibration, and solvation energy calculations were conducted with B3LYP-D3/LACVP** level of theory. Single point energies were re-evaluated with B3LYP-D3/cc-pVTZ(-f) Level of theory.

(62) Kinauer, M.; Diefenbach, M.; Bamberger, H.; Demeshko, S.; Reijerse, E. J.; Volkmann, C.; Würtele, C.; Van Slageren, J.; De Bruin, B.; Holthausen, M. C.; Schneider, S. An Iridium(III/IV/V) Redox Series Featuring a Terminal Imido Complex with Triplet Ground State. *Chem. Sci.* **2018**, *9*, 4325–4332.

Simple planar chiral catalyst
Indenyl ligand induces electronic asymmetry

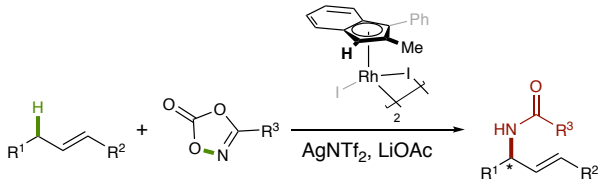

24 examples; up to 90% yield; up to 99:1 e.r.

Insert Table of Contents artwork here